Astronomical Data Analysis Software and Systems XXVI
ASP Conference Series, Vol. 521
Marco Molinaro, Keith Shortridge, and Fabio Pasian, eds.

Euclid Near-infrared Imaging Reduction Pipeline: Astrometric Calibration, Resampling and Stacking

R. da Silva,[1,2] M. Radovich,[3] A. Bonchi,[1,2] F. Faustini,[1,2] M. Frailis,[4]
G. Polenta,[1,2] R. Bouwens,[5] P. Capak,[6] K. Jahnke,[7] M. Kazandjian,[5]
X. C. Liu,[6] D. Maino,[8,9] H. Teplitz,[6] S. Wachter,[7] R. Barbier,[10] A. Ealet,[11]
B. Kubik,[10] J. Carretero,[12] E. Jullo,[13] M. Schultheis,[14] G. Seidel,[7]
S. Serrano,[15] P. Tallada,[12] and N. Tonello[12]

[1]*ASI Science Data Center, Rome, Italy;* `ronaldo.dasilva@asdc.asi.it`

[2]*INAF-Osservatorio Astronomico di Roma, Monte Porzio Catone, Rome, Italy*

[3]*INAF-Osservatorio Astronomico di Padova, Padova, Italy*

[4]*INAF-Osservatorio Astronomico di Trieste, Trieste, Italy*

[5]*Leiden Observatory, Leiden University, Leiden, Netherlands*

[6]*IPAC, Caltech, Pasadena, CA, USA*

[7]*Max-Planck-Institut für Astronomie, Heidelberg, Germany*

[8]*Dipartimento di Fisica, Università degli Studi di Milano, Milano, Italy*

[9]*INAF-Istituto di Astrofisica Spaziale e Fisica Cosmica, Milano, Italy*

[10]*INPL-Institut de Physique Nucléaire de Lyon, Lyon, France*

[11]*CPPM-Centre de Physique des Particules de Marseille, Marseille, France*

[12]*PIC-Port d'Informació Científica, Barcelona, Spain*

[13]*Aix-Marseille Université, CNRS, LAM, Marseille, France*

[14]*Laboratoire Lagrange, Observatoire de la Côte d'Azur, CNRS, Nice, France*

[15]*Institut de Ciències de l'Espai, IEEC-CSIC, Barcelona, Spain*

Abstract. Euclid is an ESA survey mission designed to understand the origin of the Universe's accelerating expansion using weak gravitational lensing and redshift clustering as main probes. Very high image quality is required for galaxy shape measurements, while accurate photometry at visible and near-infrared wavelengths and near-infrared spectroscopy are needed to measure photometric and spectroscopic galaxy redshifts. Within the Euclid Science Ground Segment, the near-infrared imaging (NIR) processing function has the task to reduce all the images produced by the near-infrared instrument (NISP) in photometric mode. Starting from Level 1 raw frames, the NIR pipeline shall produce individual images and stacked mosaics in Y, J, and H bands accounting for instrumental effects, subtracting the sky background, performing both astrometric and photometric calibrations, and providing all the information needed for catalogue production such as PSF, variance, weights, and quality flags. After an overview of the pipeline design, we present the current status of the NIR processing function development. We focus on preliminary results from the application of astrometric calibration,

resampling, and stacking procedures to simulated images, and we discuss the different approaches that we tested in order to fulfill specific requirements.

1. Introduction

The near-infrared (NIR) imaging reduction pipeline is responsibility of the NIR Organizational Unit (OU-NIR), one of the sub-projects of the Science Ground Segment (SGS) in the Euclid mission. The SGS activities are organized in Scientific Challenges (SC), each one having specific objectives in the process of deployment, installation, testing, and running of the software in development. The first preliminary version of the pipeline was released in May 2016 in the occasion of the SC#2 and includes different processing elements, or Work Packages (WP), related to some functionalities. The pipeline has been tested using data produced by the Simulations Organization Unit (OU-SIM) for the SC#2. These raw images have the Level 1 (LE1) format, which is one of the six processing levels of the SGS data products. Data were simulated for three fields (low stellar density and low zodiacal light, low stellar density and moderate zodiacal light, and high stellar density and high zodiacal light) and for three filters (Y, J, and H bands). The fields contain different pointings, each one consisting of four dithered images of 16 detectors each. These are 2k×2k detectors with 0.3″ of pixel size (which is very close to the estimated PSF, meaning an undersampling of small sources).

At the beginning of the reduction processing the LE1 input data are treated in order to homogenize the FITS structure (the WP name is Initialize Image). In this step a 3-layer frame (science, variance, and data-quality map) is created and the header is updated with the correct keywords that will be used by the other WPs. Then a mask of bad pixels is applied to the images (Bad Pixel Masking), dark current is removed (Dark Subtraction), the most energetic cosmic ray hits are detected and flagged (Cosmic Ray Rejection), and the background is calculated and subtracted (Background Subtraction). During this pre-processing of the input images, the pipeline runs in parallel for each dither. After that, the four dithers are compared with a source catalogue of reference stars and the astrometric calibration, including the modeling of the optical distortions, is performed (Astrometric Calibration). Then all dithers are resampled to a common grid (Image Resampling) and combined in one single image (Image stacking). Finally, a source catalogue is extracted from the single image (Catalog Production). Here we present the results of the astrometric calibration, resampling, and stacking steps.

2. Astrometric calibration, resampling, and stacking

The astrometric calibration is performed using SCAMP (Bertin 2006), a package of the AstrOmatic[1] software. For a given filter and pointing, the four dithers are selected for source detection using SExtractor (Bertin & Arnouts 1996), another AstrOmatic software. The extracted sources are compared with an external catalog of reference stars, produced by OU-SIM. Different catalogs corresponding to each field were used to generate the images in the Y, J, and H bands, with a magnitude limit $i \leq 24.5$ mag.

[1] `http://www.astromatic.net/software`

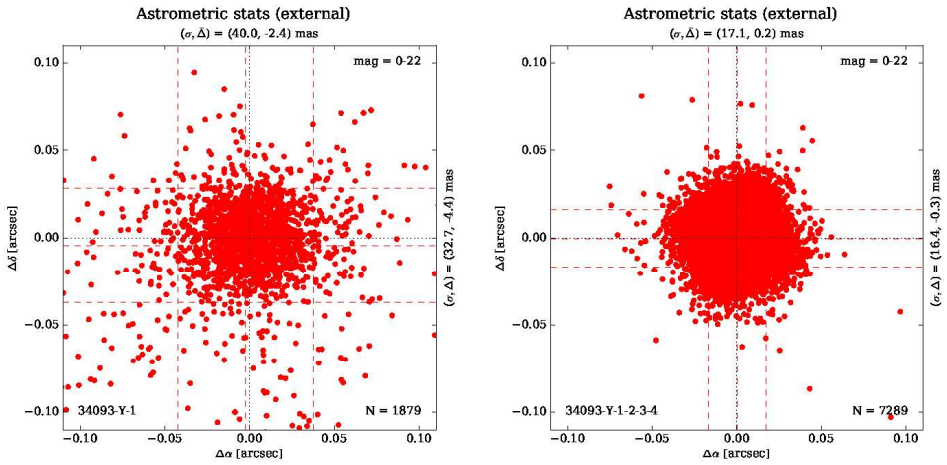

Figure 1. Differences in α and δ coordinates between detected sources and reference stars for the field Id 34093. *Left:* one filter and one dither. *Right:* one filter and four dithers. The standard deviation (σ) and mean differences ($\bar{\Delta}$), the magnitude range in the *i* band, and the number of plotted sources are also indicated.

SCAMP is run in two steps. First, we search for the placement of the focal plane by setting the parameters MOSAIC_TYPE to LOOSE and HEADER_TYPE to FOCAL_PLANE, using one dither only and writing the results in a file. Then, we use this file as input to the second step and we set MOSAIC_TYPE to SAME_CRVAL, this time using the four dithers. During the second step, a model for the optical distortions is calculated using a 3rd degree polynomial function. In the simulated images that we used the distortion pattern was assumed to be the same for all dithers and filters but, in reality, it is supposed to change for different filters and between dithers, since the distortion depends on the wavelength and on the filter wheel position. Moreover, a double Gaussian model was used to simulate the PSF shape of the sources, which has an impact in the centroid determination. The implementation of a more realistic distortion pattern and PSF is under development.

In the search for the best astrometric solution, we performed a few combinations of filters and dithers in order to find an optimal configuration. Fig. 1 shows the differences in α and δ between detected sources and reference stars (field Id 34093 - low stellar density, moderate zodiacal light) for two configurations. The standard deviations decrease from about $0.04''$ and $0.03''$ in α and δ, respectively, to about $0.017''$ and $0.016''$, and the mean differences in both coordinates are an order of magnitude smaller (within $0.0003''$ in the better case) when comparing these two cases. The conclusions for this and others fields are that all the four dithers should be used together in order to achieve a reliable astrometric solution, and that there is no need to use the three filters together if the four dithers are used. More realistic images will be produced in the next scientific challenges, which will introduce more observational noise. For the moment, we notice that the standard deviations in all cases are within $0.04''$, a factor of five smaller than the $0.2''$ accuracy settled by the Euclid SGS NIR Requirements Specification Document.

We also checked which limit in magnitude should we use for the reference stars when performing the astrometric calibration. Fig. 2 shows the internal (among dithers) and external (between detected sources and reference stars) differences in the α and δ

coordinates by setting a magnitude limit for the reference stars. The results for this and other fields indicate that an upper limit $i \leq 21$ is a good compromise in terms of having small differences in the coordinates and at the same time a number of sources large enough to provide a reliable solution for the astrometric calibration. We note that a lower limit in magnitude is set by the exclusion of saturated sources.

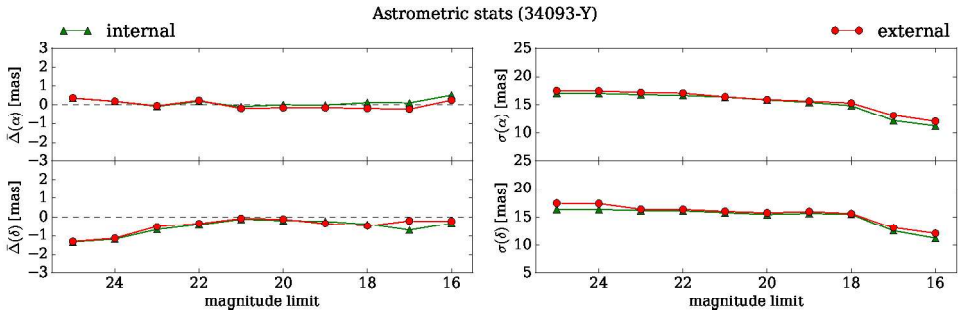

Figure 2. Internal and external standard deviations and mean differences in α and δ coordinates as a function of the magnitude limit of the reference stars used to derive the astrometric solution for the field Id 34093.

The astrometric calibrated frames of the four dithers of the same pointing and the same filter are realigned, rotated, and projected to a common grid using the SWarp (Bertin et al. 2006) AstrOmatic package. The procedure of resampling is dictated by a few parameters set in an input configuration file. One of these parameters is the RESAMPLING_TYPE, which allows the user to choose among several interpolation functions. We compare a few images (Y filter of the field Id 34093) before and after the resampling procedure by setting different interpolation functions: nearest, bilinear, and lanczos 2, 3, and 4. The "lanczos 3" function seems to be a good choice: the differences in magnitude of the extracted sources before and after resampling are within 0.02 mag for $i < 21$ mag and within 0.005 mag for $i < 19$ mag, whereas the differences in the positions are within 0.005 arcsec. The "lanczos 4" function provides differences even smaller, but may introduce larger artifacts around image discontinuities. Finally, the procedure of assembling the resampled images of single detectors is performed, also using SWarp. The parameter COMBINE_TYPE is used to the set how the individual images are combined. Again, we compared a few stacked images by setting different options, and for the moment "weighted" and "median" are those that provide the best results. For more details on the available options for the parameters used by SCAMP and by SWarp we invite the reader to have a look at the respective manuals.

Acknowledgments. We thank the Istituto Nazionale di Astrofisica (INAF) for its financial support, and the use of data and software facilities from the ASI Science Data Center (ASDC), managed by the Italian Space Agency (ASI).

References

Bertin, E. 2006, in ADASS XV, edited by C. Gabriel, C. Arviset, D. Ponz, & E. Solano, vol. 351 of ASP Conf. Ser., 4

Bertin, E., & Arnouts, S. 1996, A&AS, 117, 393

Bertin, E., et al. 2006, in ADASS XI, edited by D. A. Bohlender, C. Arviset, D. Durand, & T. H. Handley, vol. 281 of ASP Conf. Ser., 10